IIETA International Information and Engineering Technology Association
Advancing the World of Information and Engineering

Journal Européen des Systèmes Automatisés
Vol. 59, No. 2, February, 2026, pp. 513-523
Journal homepage: http://iieta.org/journals/jesa

An In-Situ Current-Voltage Characteristics Measurement System for Enhanced Performance Evaluation of Operating PV Generators

Khaoula Belguidoum*, Mahmoud Drif, Djamel Saigaa

Department of Electronics, Faculty of Technology, University of M'sila, Bordj Bou Arreridj Road, M'sila, 28000, Algeria

Corresponding Author Email: khaoula.belguidoum@univ-msila.dz

https://doi.org/10.18280/jesa.590220

Received: 29 November 2025
Revised: 28 January 2026
Accepted: 7 February 2026
Available online: 28 February 2026

Keywords:
operating photovoltaic generator, performance, telemonitoring, Arduino, Wi-Fi, IoT-Blynk application

ABSTRACT

Photovoltaic (PV) systems, like any industrial process, can be subject to various faults and anomalies during operation, which can lead to reduced performance. Effective preventive maintenance and real-time monitoring of PV installations, therefore, require early and accurate diagnostics. Although widely adopted performance analysis methods for operational PV systems, such as the widely used international standard IEC 61724, provide procedures for calculating key performance indicators, including power output, energy yield, and system efficiency. However, these approaches present notable limitations due to their narrow reliance on current and voltage measurements. Consequently, a more comprehensive and accurate performance analysis strategy is required. Direct measurement of the current–voltage (I-V) characteristic of a PV module provides significantly richer diagnostic insights and enables performance evaluation under actual operating conditions. In this context, this paper introduces a novel non-intrusive measurement approach that enables in-situ I–V characteristic measurement and real-time telemonitoring of PV generators without disconnecting or interrupting their operation. The proposed device integrates Arduino-based Wireless Mini-Characterizers (WMC), a Control Unit (CU), and a Blynk-based Graphical User Interface (GUI). The system was implemented and validated through simulation in PROTEUS. The results confirm the system's capability to perform efficient and accurate I–V curve acquisition under various operating conditions.

1. INTRODUCTION

Existing methods for performance analysis of operational photovoltaic (PV) systems, such as the widely used international standard IEC 61724 (IEC Standard 61724, 1998) [1-3], define procedures for calculating the most common performance indicators, including power output, energy yield, and system efficiency, by measuring the current and voltage at individual components within the system. However, these methods exhibit several notable limitations due to their narrow focus on current and voltage data. This limited scope may not sufficiently capture the full range of factors influencing PV system performance, potentially leading to an incomplete assessment, especially when the PV system experiences various faults and anomalies during its operation, including component failures, shading, and environmental factors such as dust and temperature. Additionally, the standard lacks comprehensive guidance on interpreting and analysing performance data, hindering efforts to pinpoint and resolve system-related issues and optimize performance.

To address this, a more precise approach to performance analysis is needed. For instance, measuring a PV module's current-voltage (I-V) characteristic serves multiple purposes, including evaluating performance under real-world conditions, facilitating maintenance, and optimizing PV system operation [4-7]. This measurement offers critical feedback for module design and helps identify potential faults. The I-V characteristic, which plots the relationship between current (I) and voltage (V) under given conditions, provides valuable insights into the module's operational health. Understanding the significance and practical applications of this measurement can greatly enhance the efficiency and reliability of solar power installations. Here are some key aspects and benefits of measuring the I-V characteristic for an operational PV array.

Firstly, the I–V characteristic is essential during the commissioning phase of a PV system, as it enables verification of the module's performance against manufacturer specifications and ensures that the installation process has not introduced any defects or faults. By measuring the I-V characteristic, engineers can detect issues such as incorrect wiring, faulty connections, or damaged cells, which might not be apparent through visual inspection alone. This initial validation helps in establishing a baseline performance metric for the system, which can be referred to in future maintenance and diagnostic activities [8].

Secondly, regular monitoring and measurement of the I–V characteristic during the operational life of a PV system significantly enhances its maintenance strategy. Deviations or shifts in the I-V characteristic over time can indicate the presence of potential problems such as shading, soiling, degradation of materials, or the onset of electrical faults [9]. For instance, a reduction in the short-circuit current (I_{sc}) might

suggest a decrease in irradiance levels due to shading or accumulation of dirt on the module surface. Similarly, changes in the open-circuit voltage (V_{oc}) could indicate thermal issues or degradation of the PV cells. By identifying these issues early, maintenance teams can take corrective actions promptly, thereby preventing more serious damage and ensuring sustained energy production.

Unfortunately, measuring the I-V characteristic of individual PV modules within a PV array without interrupting the normal operation of the system is complex but achievable using specialized equipment and techniques. To address the challenges of in-situ I-V characteristic measurement for individual PV modules in large-scale systems, this paper proposes a novel approach that minimizes disruption to overall system performance. By integrating a mini-characterizer in parallel with the module and employing a high-speed disconnection circuit with a response time of less than a few milliseconds between the PV array and the rest of the system, the module can be temporarily isolated electronically during measurement via an automated switch box and then seamlessly reintegrated into the system.

This paper is organized as follows. Section 2 presents the main categories of PV systems and provides an overview of the two most commonly used mathematical models for describing PV cell behavior. Section 3 details the proposed telemonitoring system for characterizing the complete I–V characteristics of PV modules and the PV generator, including its main components and functional architecture. A general flowchart illustrating the key steps of the telemonitoring process is also included. Section 4 describes the implementation of the proposed system on the PROTEUS platform, with control realized through a Graphical User Interface (GUI) developed using the Blynk IoT framework. Finally, Section 5 presents the experimental validation of the telemonitoring system.

2. PV SYSTEM AND PV GENERATOR MODELLING

2.1 Photovoltaic system description

A PV system is a renewable energy technology that generates electrical power by converting sunlight into electricity through PV cells. These systems can be categorized according to power capacity as residential, commercial, industrial, or utility-scale installations. Additionally, PV systems can be classified based on their connection to the electrical grid [10-13]; namely, they are broadly divided into two principal configurations: on-grid and off-grid.

2.1.1 On-grid photovoltaic system

This configuration is the most common choice for customers seeking to reduce electricity costs while relying on the utility grid as a backup during periods of insufficient solar irradiance. Two primary system types exist. A grid-connected PV system connects the PV generator directly to the utility grid through a standard inverter, without incorporating an energy storage system (Figure 1(a)). Alternatively, a utility-interactive PV system, also known as a bimodal PV system, incorporates a battery bank to store excess solar energy for later use (Figure 1(b)). These systems may be eligible for state and federal incentive programs that help offset installation costs. Grid-connected PV systems are simple to design and are very cost-effective because they have relatively few components.

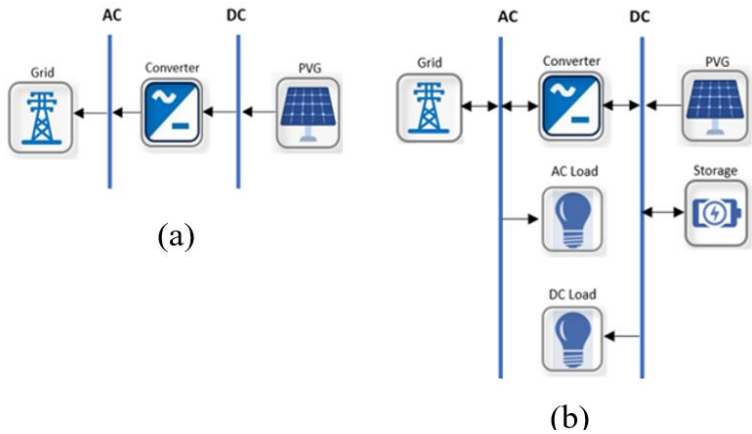

Figure 1. On-grid photovoltaic system. (a) Grid-tied system (without storage system), (b) Utility-interactive photovoltaic (PV) system (with storage system)

2.1.2 Off-grid photovoltaic system

An off-grid PV system is an independent power generation system that operates without a connection to the electrical grid, making it suitable for customers in remote areas or those seeking energy independence. Unlike grid-tied systems, off-grid systems rely solely on solar power as the primary energy source. Excess electricity generated is stored in batteries for use during periods of low solar generation or at night. Two primary system configurations are commonly used: standalone and hybrid systems. A standalone PV system, as depicted in Figure 2(a), operates independently of the electrical grid. It primarily consists of PV modules that convert sunlight into direct current (DC) electricity. To ensure a continuous power supply, especially during periods of low sunlight, this electricity is stored in batteries. An inverter then converts the stored DC power into AC power compatible with most household appliances. The other common type of off-grid system is the "Hybrid PV System", as illustrated in Figure 2(b), which is essentially a standalone PV system augmented with additional energy sources, such as wind turbines, diesel generators, hydro turbines, or fuel cells, to ensure a continuous supply of energy regardless of prevailing weather conditions.

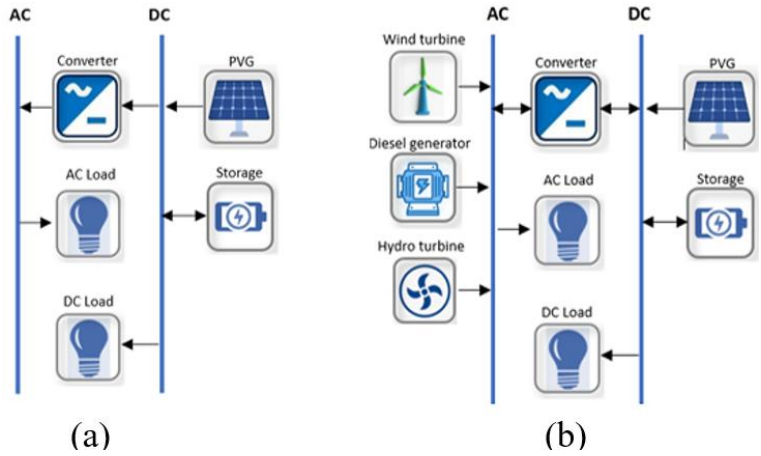

Figure 2. Off-grid photovoltaic system. (a) Standalone photovoltaic (PV) system, (b) Hybrid PV system

2.2 PV generator modelling

Among the various components that constitute the PV system, such as the storage system, inverter, and more, the PV generator (PVG) stands out as a critical element. It typically represents the largest share of the overall system from an economic point of view. A PVG is a complete power-generating unit that consists of multiple interconnected PV modules, working together to convert sunlight into electrical energy for various applications. There are four well-known types of PVG configurations [14, 15]: Series-Parallel (SP), Bridge-Linked, and Total-Cross-Tied (TCT), as shown in Figure 3. In a PV module, PV cells are connected in a series and parallel configuration, depending on the desired voltage and current characteristics.

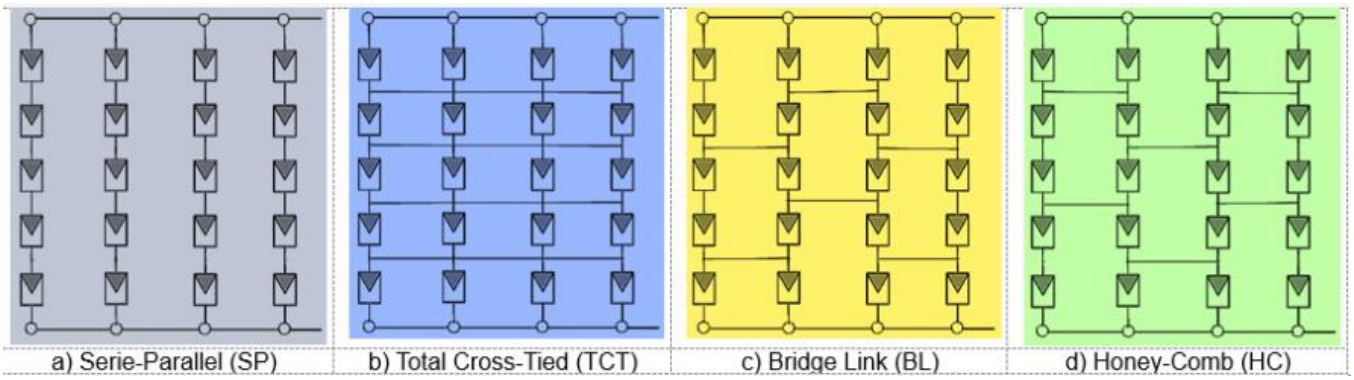

Figure 3. Typical configurations of a photovoltaic generator (5 × 4)

As previously mentioned, to simulate and assess the performance of this critical component, we employ the comprehensive I-V characteristics of the PV modules, which offer valuable insights into module health. Essentially, this involves utilizing a mathematical model of the PV generator to predict its behaviour under diverse operating conditions. In this context, two classic models are commonly employed: the Single Diode Model (SDM) and the Double Diode Model (DDM) [16, 17]. The SDM, also known as the five-parameter model, is the most widespread model used for PV cells and PV modules due to its low complexity and good accuracy in power generation. Similarly, the DDM, also known as the seven-parameter model, offers a good compromise between complexity and accuracy, achieving higher precision. In this regard, both models are invaluable tools for understanding and predicting the performance of PV systems.

According to the electrical equivalent circuits of PV cells depicted in Figure 4, the expressions of the single exponential model (SDM) and the double exponential model (DDM) can be summarized by the implicit function in Eq. (1). To use the single exponential model, set n = 1, and to use the double exponential model, set n = 2.

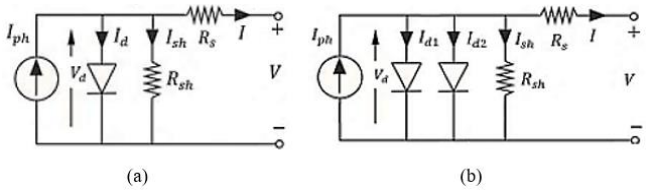

Figure 4. Equivalent-circuit models of PV cell: (a) Single Diode Model (SDM), (b) Double Diode Model (DDM)

$$I = I_{ph} - \sum_{i=1}^{n} I_{oi} \left[exp\left(q \frac{V + R_S I}{A_i k T} \right) - 1 \right] - \frac{V + R_S I}{R_{sh}} \quad (1)$$

In this equation I_{ph}, R_s, R_{sh}, I_{oi}, and A_i are the parameters of the model, which are related to the internal properties of the PV cell. They denote the light-generated current (or photocurrent), the series resistance, the shunt resistance, the reverse saturation current of the diode, and the ideality factor. The rest of the known parameters are the Boltzmann constant (k = 1.3806503 × 10^{-23} J/K), the electron charge (q = 1.60217646 × 10^{-19} C), and the temperature of the junction in Kelvin. It is worth noting that the SDM contains five undetermined parameters, namely, I_{ph}, R_s, R_{sh}, R_s, I_{oi}, while

the DDM includes seven undetermined parameters, i.e., I_{ph}, R_s, R_{sh}, R_s, I_{oi}, A_1, and A_2. To further simplify the DDM, several researchers have considered that ($A_1 = 1$) and ($A_1 = 2$), which leads to a decrease in the number of parameters to 5. Regarding the PV module as the fundamental building block of a PV generator, it is crucial in determining the system's voltage and power output. Commercial PV modules typically comprise (n_p) strings of series-connected cells (n_s), arranged in parallel. To accurately model the module's behavior, we can derive its characteristics from the individual cell model (Eq. (1)), as illustrated in the following expression (Eq. (2)).

$$I = n_p I_{ph} - n_p \left(\sum_{i=1}^{n=2} I_{oi} \left[exp\left(q \frac{V + \left(\frac{n_s}{n_p}\right) R_s I}{n_s A_i k T} \right) - 1 \right] \right) - \frac{V + \left(\frac{n_s}{n_p}\right) R_s I}{\left(\frac{n_s}{n_p}\right) R_{sh}} \quad (2)$$

In order to determine the PV cell outputs (current and voltage) and thus the power that can delivered by the PV module under an arbitrary operating condition, we must use additional equations that express each of the model parameters (I_{ph}, R_s, R_{sh}, R_s, I_{oi} and A_i) as a function of cell temperature (T) and total absorbed irradiance (G), as illustrated in the following equations:

$$I_{ph} = (I_{ph}^* + \mu_{Isc}(T - T^*)) \frac{G}{G^*} \quad (3)$$

$$I_{oi} = I_{oi}^* \left(\frac{T}{T^*}\right)^3 \exp\left[\frac{q\, E_g}{A_i k}\left(\frac{1}{T} - \frac{1}{T^*}\right)\right] \quad (4)$$

$$R_s = R_s^* \quad (5)$$

$$R_{sh} = \left(\frac{G^*}{G}\right) R_{sh}^* \quad (6)$$

$$A_i = A_i^* \quad (7)$$

In the above equations I_{ph}^* ($\approx I_{sc}^*$), I_{oi}^* , R_s^*, R_{sh}^* and A_i^* represent the model parameters typically provided by the manufacturer as data valid under Standard Test Conditions (STC) of a spectrum of AM 1.5, an irradiance of G^*=*1000 W.m*$^{-2}$, and a cell temperature of T^* = 25 °C. Regarding the model selection in this study, while the Double Diode Model (DDM) can offer enhanced precision under specific operating conditions, the Single Diode Model (SDM) remains a widely accepted standard in the literature due to its reliable accuracy and reduced computational overhead. Within the framework of this research, the most critical factor is the ultra-fast execution of the I–V curve measurement to ensure it does not negatively impact the PV system's operation. Given that the priority is to maintain system continuity through a disconnection time of less than 300 ms, the computational efficiency of the SDM is highly advantageous. This choice allows for rapid parameter identification without the high mathematical complexity of the DDM, ensuring that the diagnostic process remains non-intrusive and results in statistically negligible energy loss.

3. THE PROPOSED TELEMONITORING SYSTEM

We acknowledge that in-situ measurements of the full I-V curve for an individual PV module within a large photovoltaic generator (PVG), without isolating it from its string (i.e., while it remains integrated) and without interrupting the system's regular operation, are complex, if not nearly impossible, and notably challenging. This complexity primarily arises from the interference caused by other modules and current flow interference; that is, when a module is part of a series string, the current flowing through it is influenced by its neighbours in the string.

To address the challenges of in-situ I-V characteristic measurement for individual PV modules within large-scale systems, this paper proposes a novel approach. By integrating a mini-characterizer in parallel with the module and employing a high-speed disconnection circuit, we can accurately measure the module's I-V characteristic while maintaining uninterrupted system operation. This method involves isolating the PV generator from the system for less than 20 milliseconds. Additionally, to mitigate potential interference between modules in different strings, blocking diodes are incorporated at the output of each string, regardless of the PV generator (PVG) configuration—whether it is Series-Parallel (SP), Total-Cross-Tied (TCT), Bridge-Linked (BL), or Honey-Comb (HC).

Based on the proposed approach outlined above, we suggest a telemonitoring system for PV modules. As illustrated in Figure 5, this system comprises four primary components: the Wireless Mini-Characterizer (WMC), the Data Acquisition and Control Unit (ADCU), the Wireless Digital Switch that connects the PVG to the rest of the PV system (WDS-G), and the GUI.

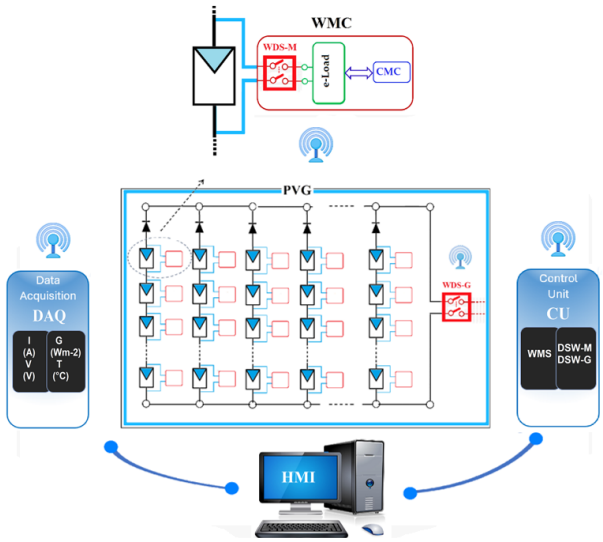

Figure 5. Functional block diagram of the proposed telemonitoring system

3.1 Wireless digital switch

To accurately capture the full, I–V characteristic of a PV module without disturbing normal operation, a high-speed switching circuit that temporarily decouples the module from the system is used. This operation is controlled by the Central Unit (CU) via a Wireless Digital Switch (WDS-G) at the start and end of each measurement.

3.2 Wireless mini-characterizer

Each PV module is equipped with a Wireless Mini-

Characterizer (WMC). In the proposed system, communication is enabled via Wi-Fi, activated by the Control Unit (CU). The WMC incorporates an internal isolation circuit, known as a Digital Switch (DWS), which temporarily connects to the module during measurements when activated by a logic level '1' signal transmitted by the Circuit Measuring Control (CMC). To capture the module's I-V characteristic, the WMC uses a DC/DC converter that functions as an electronically controlled load [18-20]. This converter is controlled by the CMC, which dictates the precise steps of resistance change. By progressively increasing the load resistance, the converter sweeps through the module's I-V characteristic, starting from the short-circuit current (I_{sc}) point and ending at the open-circuit voltage (V_{oc}) point.

3.3 Control unit

The CU, based on an Arduino board [21, 22], plays a crucial role in preparing the system for measurement. Before initiating the process, it activates the disconnection circuit (WDS-G) to isolate the PVG from the rest of the PV system. To measure individual or multiple modules simultaneously, it then orders the corresponding WMCs to take measurements. Once the measurements are complete, it deactivates the PVG disconnection and captures the readings for analysis and display.

3.4 Graphical User Interface

The GUI serves as the primary interface between the user and the PV system's telemonitoring system. It is designed using the IoT Blynk application [23, 24]. This interface allows users to configure monitoring options such as selecting specific modules or the entire PV generator for testing, and setting the number of sequences. It also enables users to receive I-V curve data and climatic parameters and analyze them through visual representations. Essentially, the GUI acts as the command centre for overseeing and managing the PV system's telemonitoring.

As described in previous sections, the telemonitoring system consists of four primary components. These are dedicated to measuring the outdoor and in-situ I-V characteristics of PV modules within a PV generator, along with the operating condition parameters such as irradiance and temperature. The following section and the flowchart in Figure 6 provide a detailed explanation of the measurement procedure for a single module using this proposed method.

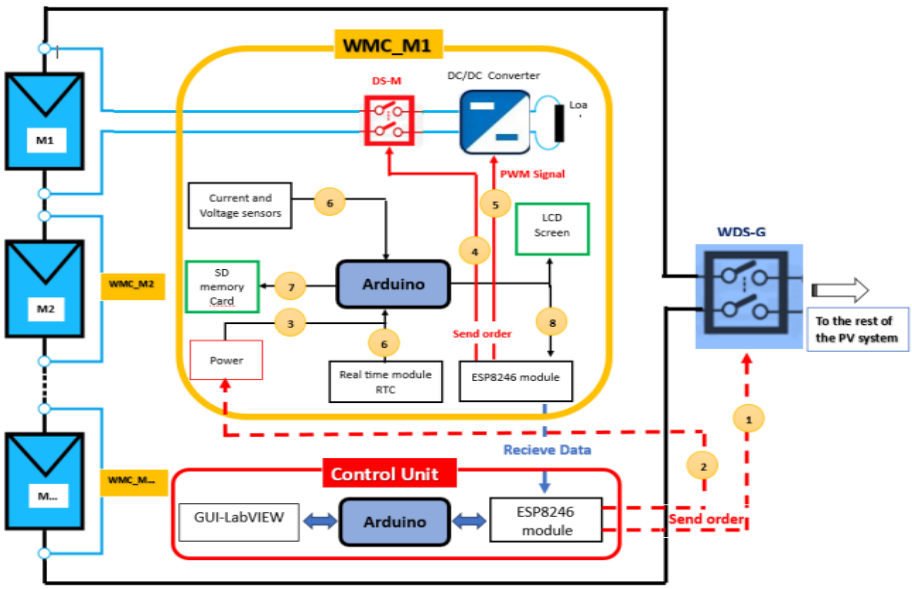

Figure 6. Main steps for measuring the I-V characteristic in-situ of a single module using the proposed system

4. IMPLEMENTATION OF THE PROPOSED TELEMONITORING SYSTEM IN PROTEUS

To simulate a telemonitoring and control system for a PV system within the PROTEUS environment, we created a virtual representation of its physical components. This involved utilizing PROTEUS' built-in libraries or developing custom models for the PV modules, characterizer circuitry, and associated elements such as load resistors, current, and voltage sensors. Additionally, PROTEUS offers a comprehensive library for modelling a wide range of practical microcontrollers, unlike other simulation programs like MATLAB, PSCAD, and PSIM that require separate modelling of the controller circuit.

Initially, we implemented a PV module model based on the widely used Single Diode Model (SDM), as defined in Eqs. (1)-(7). To enhance the model's integration into various applications, a masked model with its own dialog box parameters was created, as shown in Figure 7. In the PV module block, the output port V+ represents the positive terminal PV (+), and the output port V- represents the negative terminal PV (-). The input ports TEMP and IRRAD are used for irradiance and cell temperature, respectively. Additionally, we developed a wireless mini-characterizer (WMC), as illustrated in Figure 8, designed for in-situ measurement of the I-V characteristic of any PV module integrated into the PV system. The electronic load is a boost-type DC/DC converter controlled by the microcontroller on the Arduino board, as depicted also in Figure 8. On the other hand, we implemented a CU, based on an Arduino board, which remotely controls the entire system via Wi-Fi communication.

User interaction is facilitated through a graphical user interface (Blynk GUI), the platform of which is described in Figure 9. This interface allows the operator to select specific modules or the entire PV generator for characterization, as well as the measurement time.

Blynk GUI is a low-code IoT platform that provides a ready-to-use cloud infrastructure for connecting electronic devices for remote monitoring and control, requiring only an ESP32 or Raspberry Pi to connect to the device, while also enabling the rapid creation of interactive mobile applications.

It can be divided into three main elements: With Blynk.Cloud, Blynk.Apps, Blynk.Console.

- Blynk Cloud (The Core): This is the central server that receives data from sensors (via Wi-Fi, cellular, etc.), stores it, and transmits it to the mobile or web applications. It manages authentication and data streams.
- Blynk App (Mobile Interface): A no-code app builder for creating custom touch interfaces on a mobile phone (buttons, gauges, graphs) to control and monitor your PV system in real time, directly from the cloud.
- Blynk Console (The Web Interface): A web console for higher-level management: creating templates for new devices, managing users, historical data, and advanced configuration, providing an overview of the IoT fleet.

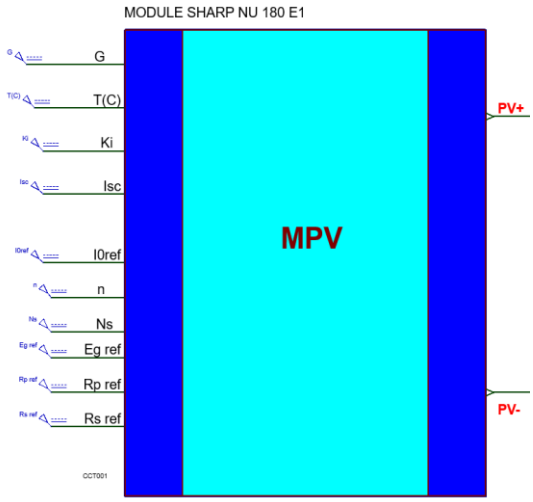

Figure 7. Developed photovoltaic (PV) module model for PROTEUS

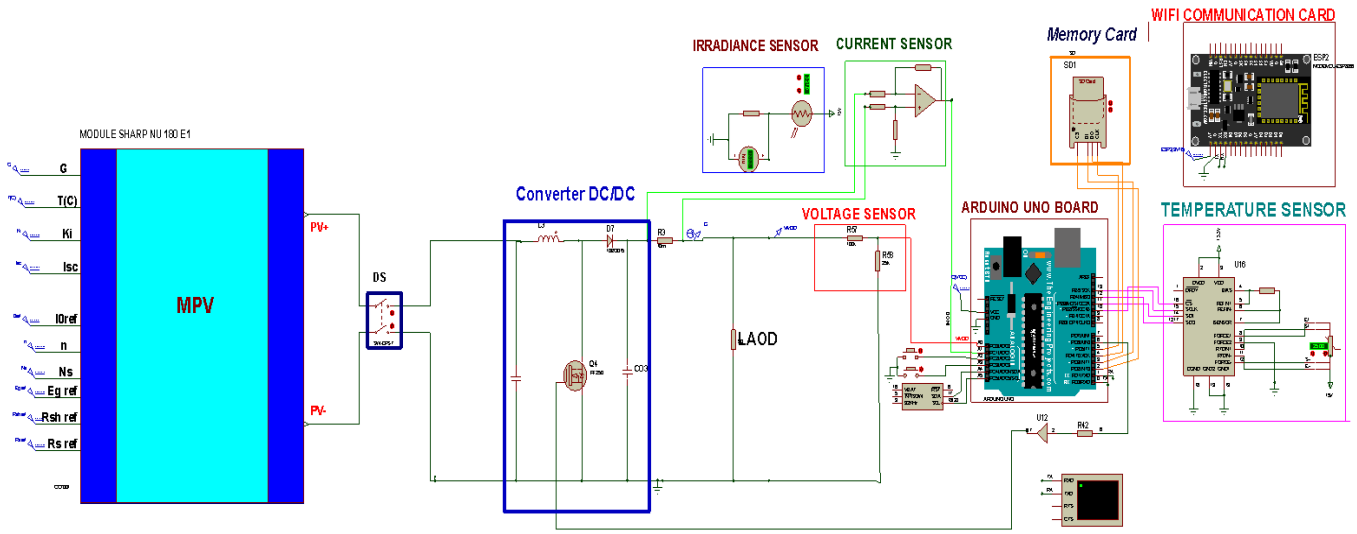

Figure 8. Photovoltaic (PV) module characterizer implementation in PROTEUS

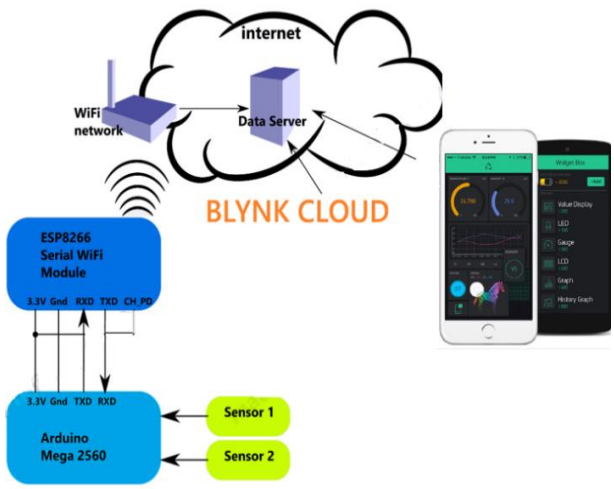

Figure 9. Main elements of Blynk Graphical User Interface (GUI)

For telemonitoring of the photovoltaic system, the microcontroller (ESP32) connects to the Blynk.Cloud, exchanging data via virtual pins (Data streams). The Blynk Cloud then publishes this data to the Console (for analysis) and makes it available to the mobile app via the configured Data streams. Finally, clicking a button in the app or console sends a command via the cloud to the WDS-G, for example, which then executes the action (e.g., turning on an LED).

5. SIMULATION AND RESULTS

This section validates the proposed method. A simulation study was carried out on the SHARP NU-180(E1) PV module under uniform irradiance conditions (identical irradiance applied to all modules) and non-uniform irradiance conditions (partial shading). The module consists of 48 monocrystalline silicon cells arranged in 6 rows and 12 columns. The electrical parameters under Standard Test Conditions (STC: 1000 W/m², 25 °C) are listed in Table 1. As a case study, a PV generator

with a 2 × 3 series–parallel module configuration was implemented, as shown in Figure 10.

This study investigated two operating scenarios. In the first, all modules operated under a uniform irradiance of 800 W/m² at 38 °C. The second scenario examined partial shading conditions where irradiance was non-uniform: modules M (1,1), M (1,3), and M (2,1) received 900 W/m², while M (1,2), M (2,2), and M (2,3) were exposed to 600 W/m², 500 W/m², and 300 W/m², respectively.

To reconstruct the I-V characteristics of individual modules or the entire PV generator (PVG), data are acquired via real-time measurements. These data are transmitted through Wi-Fi from the Proteus-based characterizer to the Blynk monitoring and control platform, where they can be visualized on a mobile device or PC.

As illustrated by the current and voltage profiles over time in Figures 11 and 12, the real-time data transfer for a single PV module requires approximately 50ms. While the raw transmission between the sensor and the controller occurs in a fraction of a second, the total latency observed in the plots encompasses the physical system response, data processing, and storage time. Consequently, 50 ms is established as the response time per individual module. To evaluate all units within the generator and ensure optimal operational efficiency, the total measurement cycle is completed in approximately 300 ms.

Table 1. Manufacturer parameters of SHARP NU-180(E1) photovoltaic (PV) module at STC (1000 W/m², 25 °C)

Parameters	Values
Technology	Si-mono
Maximum power, P_m	180 W
Voltage at P_m, V_m	23.70 V
Current at P_m, I_m	7.6 A
Short-circuit current, I_{sc}	8.37 A
Open-circuit voltage, V_{oc}	30.00 V
Ideality factor, A	1.128
Diode saturation current, I_o	$3{,}4710^{-9}$ A
Shunt resistance, R_{sh}	150 Ω
Series resistance, R_s	0.35 Ω
Temperature coefficient of open circuit voltage, k_{Voc}	-48 mV/°C
Temperature coefficient of short-circuit current, k_{Isc}	4.43 mA/°C
Number of cells in series	48
Number of cells in parallel	1

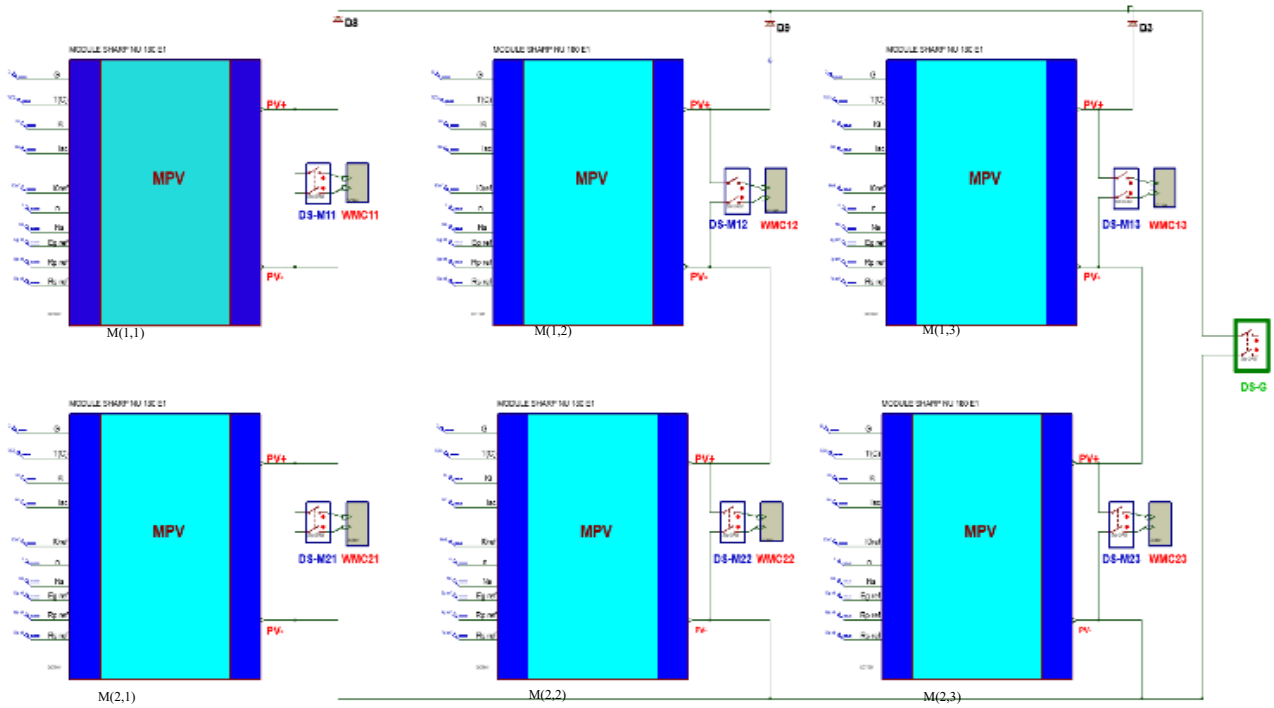

Figure 10. PV generator of 2 × 3 series-parallel configuration in PROTEUS

Regarding the simulation results for the individual modules and the corresponding generator under the two scenarios (uniform irradiance and non-uniform conditions), the recorded I-V characteristics are displayed in Figures 13-16. It is important to emphasize that the developed telemonitoring system is capable of capturing these characteristics regardless of the irradiance distribution across the module plane.

Furthermore, the entire diagnostic process for the set of six modules, including the full generator, is completed in less than 300 ms. This duration represents the total time the PV generator is disconnected from the rest of the system; as this window is extremely brief, it ensures that the overall system operation and energy production remain unaffected.

The accuracy of the reconstructed I-V characteristics is influenced by several hardware and acquisition factors, primarily sensor precision and data sampling limitations. The current and voltage sensing circuits, employing resistive dividers and shunts, typically provide a base accuracy of ± 0.5%. However, these components can be subject to precision degradation due to thermal drift and operational nonlinearity. Additionally, the use of low-power microcontrollers (such as the Arduino or ESP32) introduces quantization errors during the analog-to-digital conversion (ADC) process, particularly when the resolution is limited to 10 or 12 bits.

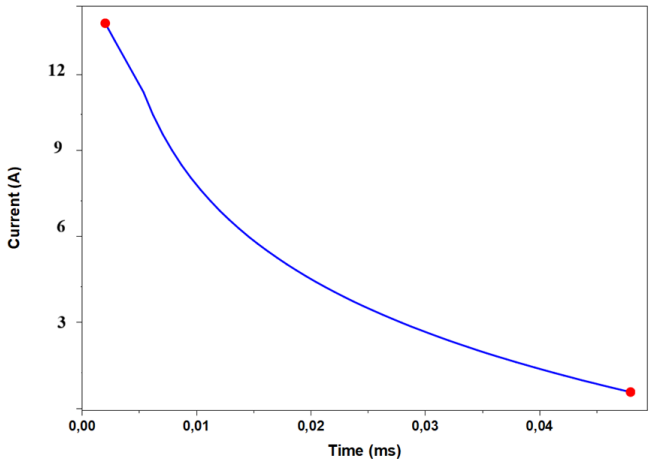

Figure 11. Real-time current measurement for the PV generator

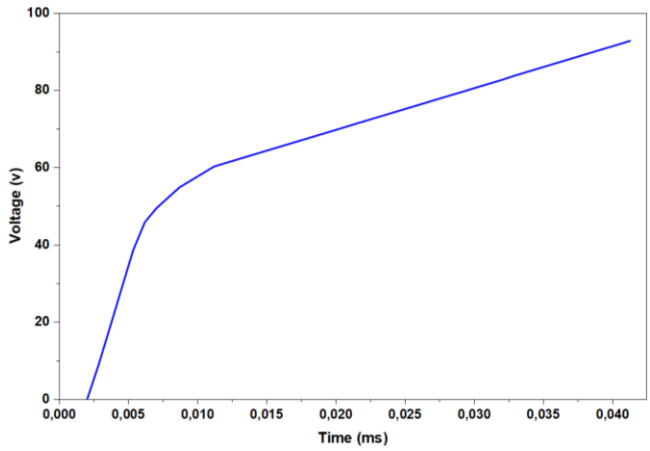

Figure 12. Real-time voltage measurement for the PV generator

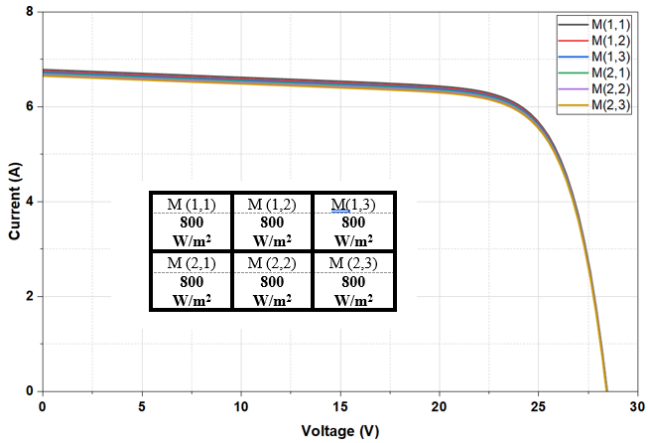

(a)

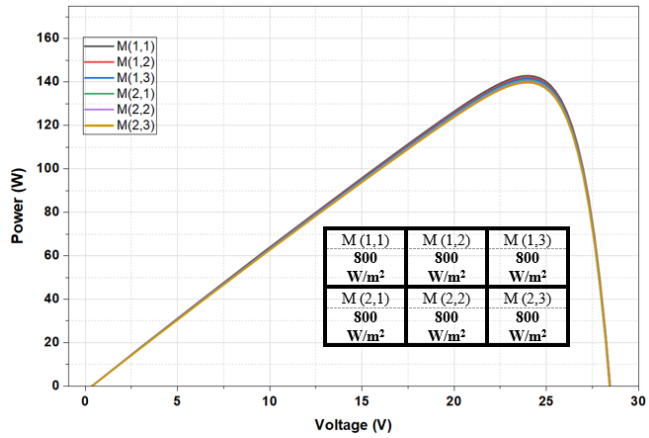

(b)

Figure 13. I-V and P-V characteristics for the 6 modules under the same weather conditions: 800 W/m^2 and 38 °C
Note: The obtained parameters for each module are: V_m = 24 V, I_m = 6 A, P_m = 144 W

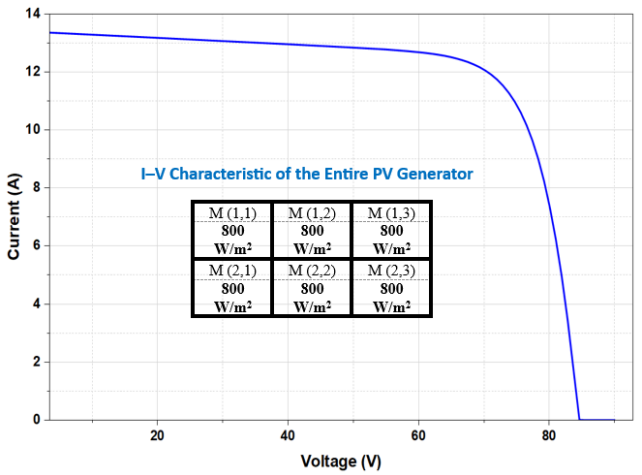

(a)

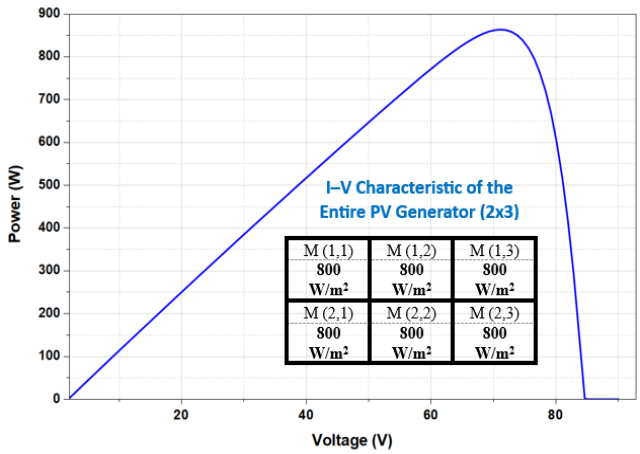

(b)

Figure 14. Characteristics for the entire PV generator under the weather conditions: 800 W/m^2 and 38 °C. (a) I-V characteristic, (b) P-V characteristic
Note: The obtained parameters are: V_{ocG} = 85.5V, I_{scG}= 13.54A, V_{mG} = 72.0 V, I_{mG} = 12 A, P_{mG} = 864 W

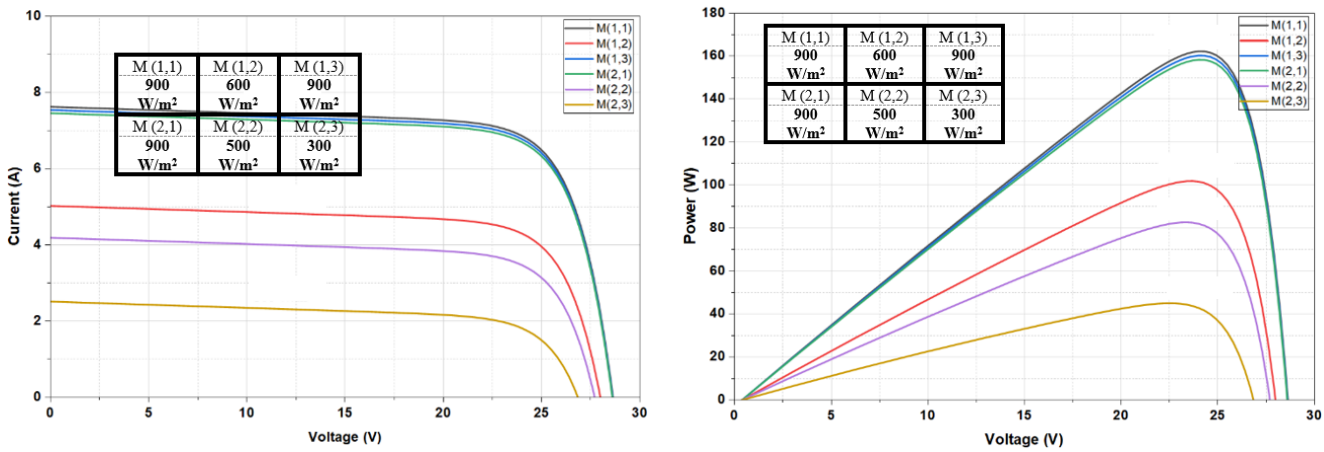

Figure 15. I-V and P-V characteristics for the 6 modules under different weather conditions

Note: For M(1,1), M(1,3), and M(2,1): V_{oc} = 28.60V, I_{sc} = 7.51 A, V_m = 24.40 V, I_m = 6.65 A, P_m = 161 W, For M(1,2): V_{oc} = 28 V, I_{sc} = 5 A, V_m = 24.00 V, I_m = 4.29 A, P_m = 103 W, For M(2,2): V_{oc} = 27.70 V, I_{sc} = 4.19 A, V_m = 23.40 V, I_m = 3.51 A, P_m = 82.30 W, For M(2,3): V_{oc} = 26.80 V, I_{sc} = 2.50 A, V_m = 22.25 V, I_m = 2 A, P_m = 44.5 W

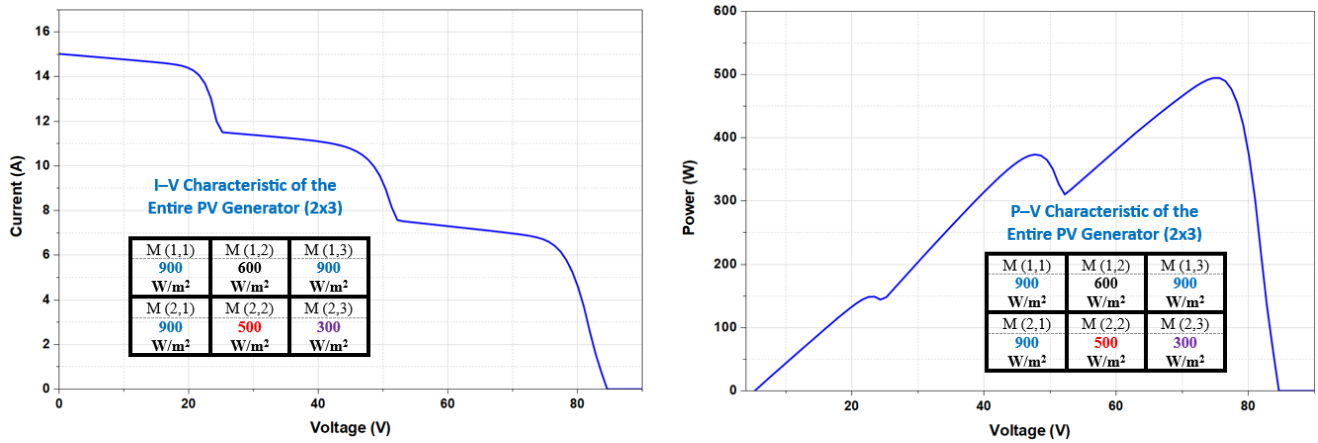

(a) (b)

Figure 16. I-V and P-V characteristics for the entire PV generator under non-uniform weather conditions

Furthermore, the relationship between the sampling rate and the characterization sweep speed is a critical determinant of data fidelity. An insufficient sampling frequency can lead to the loss of key inflection points on the I-V curve or introduce dynamic distortion and aliasing. In this study, the measurement window is set to approximately 300ms, providing a sufficiently slow sweep to allow for accurate digitization. By utilizing a sampling frequency of 1 kHz, the system captures 300 discrete points per curve. This high data density effectively minimizes aliasing and dynamic error, ensuring a high-fidelity representation of the PV module's performance under both uniform and non-uniform irradiance conditions.

On the other hand, to quantitatively assess the impact of the ultra-fast measurement on the PV generator's performance, we consider a single measurement cycle with a disconnection duration of 300 ms. For a module operating at a steady power, the energy loss per measurement is the product of that power and the disconnection time.

To determine what this loss represents relative to the total daily production, we assume a standard 10-hour production day at a steady average power. Under these conditions, the relative energy loss for a single 300 ms measurement is approximately 0.00083%.

Even if the diagnostic is performed hourly (10 times a day), the total cumulative loss would be approximately 0.0083%. This value is several orders of magnitude smaller than the typical accuracy of industrial power meters (usually between ± 0.5 and 2%) and the fluctuations caused by minor atmospheric variations. Consequently, the disconnection has a negligible quantitative impact on the overall energy yield of the PV system.

6. CONCLUSIONS

A novel approach to assess the performance of a photovoltaic system, and precisely on the photovoltaic generator, has been proposed. This method involves real-time telemonitoring to measure the I-V curves of both individual photovoltaic modules and the entire generator, without disrupting the normal operation of the system. In this context, we have developed a novel, portable device capable of low-cost I-V characteristic measurement and real-time telemonitoring of photovoltaic systems. The monitoring process uses a more affordable electronic device to measure the complete characteristics of the module within a string. This device, called a wireless mini-characterizer (WMC), is connected in parallel with the module and can be remotely controlled.

The telemonitoring system is based on three main independent elements: the Wireless Mini-Characterizer

(WMC), the Wireless Digital Switch (WDS) that connects the photovoltaic generator to the rest of the photovoltaic system, and the CU that controls the first two elements and receives remote measurement data. This system has been implemented on the circuit-oriented software platform PROTEUS, with control and visualization achieved through a GUI developed using the IoT Blynk application. Encouraging preliminary results from simulations demonstrate the feasibility of the proposed approach.

The variations recorded in the energy production by the panels over time represent a major challenge to verify their safety, but with this device, we can achieve this due to its ease of installation and maintenance if it is damaged, and at a low cost.

In this work, only numerical simulation results were relied upon, and experimental testing for model validation has not yet been conducted due to time and resource constraints. For future work, we plan to develop a prototype of this telemonitoring system, reduce the measurement time, and validate it experimentally on a real photovoltaic system.

Regarding the system's scalability, the modular nature of the proposed high-speed switching circuit allows for expansion across larger photovoltaic generators (PVG). The architecture is capable of measuring multiple arrays in parallel by duplicating the sensing and switching units across various strings. When integrated with a multi-channel synchronization controller, the system can perform simultaneous I-V characterization of multiple modules or arrays. This parallelization ensures that comprehensive plant-level diagnostics can be achieved while maintaining the ultra-fast, non-intrusive operational standards demonstrated in this work.

ACKNOWLEDGMENT

My sincere thanks go to my thesis supervisor, Dr. Mahmoud Drif. His unwavering support and invaluable guidance were instrumental in every stage of this project.

REFERENCES

[1] Eltawil, M.A., Zhao, Z. (2010). Grid-connected photovoltaic power systems: Technical and potential problems. A review. Renewable and Sustainable Energy Reviews, 14(1): 112-129. https://doi.org/10.1016/j.rser.2009.07.015

[2] Okello, D., Van Dyk, E.E., Vorster, F.J. (2015). Analysis of measured and simulated performance data of a 3.2 kWp grid-connected PV system in Port Elizabeth, South Africa. Energy Conversion and Management, 100: 10-15. https://doi.org/10.1016/j.enconman.2015.04.064

[3] Neeraj, K. (2022). Chapter 16 - Online condition monitoring and maintenance of photovoltaic system. System Assurances. Modelling and Management. Emerging Methodologies and Applications in Modelling System Assurances, 287-305. https://doi.org/10.1016/B978-0-323-90240-3.00016-3

[4] Augusto, A., Killam, A., Bowden, S.G., Wilterdink, H. (2022). Measuring outdoor I–V characteristics of PV modules and systems. Progress in Energy, 4(4): 042006. https://doi.org/10.1088/2516-1083/ac851c

[5] Parra-Quiroga, J.S., Franco-Mejía, É., Orozco-Gutiérrez, M.L., Bastidas-Rodríguez, J.D. (2022). Performance comparison of electrical indicators for detection of PID in PV panels. Revista UIS ingenierías, 21(3): 21-32. https://doi.org/10.18273/revuin.v21n3-2022003

[6] Li, B., Migan-Dubois, A., Delpha, C., Diallo, D. (2020). Analysis of the performance of the IV curve correction methods in the presence of defects. In 37th European Photovoltaic Solar Energy Conference and Exhibition (EU PVSEC 2020)**,** Lisbon, Portugal, pp. 1-5. http://doi.org/10.4229/EUPVSEC20202020-5CV.3.54

[7] Van Dyk, E.E., Gxasheka, A.R., Meyer, E.L. (2005). Monitoring current–voltage characteristics and energy output of silicon photovoltaic modules. Renewable Energy, 30(3): 399-411. https://doi.org/10.1016/j.renene.2004.04.016

[8] Luque, A., Hegedus, S. (2011). Handbook of photovoltaic science and engineering. John Wiley & Sons.

[9] Osmani, K., Haddad, A., Lemenand, T., Castanier, B., Alkhedher, M., Ramadan, M. (2023). A critical review of PV systems' faults with the relevant detection methods. Energy Nexus, 12: 100257. https://doi.org/10.1016/j.nexus.2023.100257

[10] Oprea, S.V., Bâra, A. (2024). On-grid and off-grid photovoltaic systems forecasting using a hybrid meta-learning method. Knowledge and Information Systems, 66(4): 2575-2606. https://doi.org/10.1007/s10115-023-02037-8

[11] Morey, M., Gupta, N., Garg, M.M., Kumar, A. (2023). A comprehensive review of grid-connected solar photovoltaic system: Architecture, control, and ancillary services. Renewable Energy Focus, 45: 307-330. https://doi.org/10.1016/j.ref.2023.04.009

[12] Karthikeyan, V., Rajasekar, S., Das, V., Karuppanan, P., Singh, A.K. (2017). Grid-connected and off-grid solar photovoltaic system. In Smart Energy Grid Design for Island Countries: Challenges and Opportunities, pp. 125-157. https://doi.org/10.1007/978-3-319-50197-0_5

[13] Mandelli, S., Barbieri, J., Mereu, R., Colombo, E. (2016). Off-grid systems for rural electrification in developing countries: Definitions, classification and a comprehensive literature review. Renewable and Sustainable Energy Reviews, 58: 1621-1646. https://doi.org/10.1016/j.rser.2015.12.338

[14] Rajani, K., Ramesh, T. (2022). Reconfiguration of PV arrays (TCT, BL, HC) considering wiring resistance. CSEE Journal of Power and Energy Systems, 8(5): 1408-1416. https://doi.org/10.17775/CSEEJPES.2020.06930

[15] Al Mansur, A., Amin, M.R., Islam, K.K. (2019). Determination of module rearrangement techniques for non-uniformly aged PV arrays with SP, TCT, BL and HC configurations for maximum power output. In 2019 International Conference on Electrical, Computer and Communication Engineering (ECCE), Cox'sBazar, Bangladesh, pp. 1-5. https://doi.org/10.1109/ECACE.2019.8679176

[16] Drif, M., Bouchelaghem, A., Guemache, A., Benhamadouche, D.A., Saigaa, D. (2024). A novel method to obtain reverse bias I–V curves for single cells integrated in photovoltaic modules. Power Electronics and Drives, 9: 412-427. http://doi.org//10.2478/pead-2024-0027

[17] Drif, M., Bahri, M., Saigaa, D. (2021). A novel equivalent circuit-based model for photovoltaic sources. Optik, 242: 167046.

https://doi.org/10.1016/j.ijleo.2021.167046
[18] Durán, E., Andújar, J.M., Enrique, J.M., Perez-oria, J.M. (2012). Determination of PV generator IV/PV characteristic curves using a DC-DC converter controlled by a Virtual Instrument. International Journal of Photoenergy, 1: 843185. https://doi.org/10.1155/2012/843185
[19] Duran, E., Piliougine, M., Sidrach-de-Cardona, M., Galan, J., Andujar, J.M. (2008). Different methods to obtain the I–V curve of PV modules: A review. In 2008 33rd IEEE Photovoltaic Specialists Conference, San Diego, CA, USA, pp. 1-6. https://doi.org/10.1109/PVSC.2008.4922578
[20] Duran, E., Galán, J., Sidrach-de-Cardona, M., Andujar, J.M. (2007). A new application of the buck-boost-derived converters to obtain the IV curve of photovoltaic modules. In 2007 IEEE Power Electronics Specialists Conference, Orlando, FL, USA, pp. 413-417. https://doi.org/10.1109/PESC.2007.4342022
[21] Azi, A.A., Saigaa, D., Drif, M., Loukriz, A. (2024). Development of generalized photovoltaic model using ISIS-PROTEUS. Studies in Engineering and Exact Sciences, 5(2): e5546-e5546. https://doi.org/10.54021/seesv5n2-015
[22] Motahhir, S., Chalh, A., El Ghzizal, A., Sebti, S., Derouich, A. (2017). Modeling of photovoltaic panel by using proteus. Journal of Engineering Science and Technology Review, 10: 8-13. https://doi.org/10.25103/jestr.102.02
[23] Abd Razak, T.M.F.B. (2023). Real time monitoring small scale off grid solar system with Blynk App. Progress in Engineering Application and Technology, 4(2): 385-393. https://doi.org/10.30880/peat.2023.04.02.037
[24] Jie, L. W., Sen, T.P., Ghani, N.M.A., Abas, M.F. (2021). Automatic control of color sorting and pick/place of a 6-DOF robot arm. Journal Européen des Systèmes Automatisés, 54(3): 435-443. https://doi.org/10.18280/jesa.540306

NOMENCLATURE

Symbols

A_i	diode ideality factor
A^*_i	diode ideality factor under STC
Eg	energy gap of the cell material
G	irradiance (W/m^2)
G^*	reference irradiance (often $1000W/m^2$)
I	current (A)
Isc	short-circuit current (A)
I_{ph}	light-generated current (A)
I_{ph}^*	light-generated current under STC (A)
I_{oi}	reverse saturation current of diode at temperature T
I_{oi}^*	reverse saturation current of diode under STC
K	Boltzmann constant (J/K)
q	electron charge (C)
R_s	series resistance (**Ω**)
R_s^*	series resistance under STC (**Ω**)
R_{sh}	shunt resistance (**Ω**)
R_{sh}^*	shunt resistance under STC (**Ω**)
T	temperature (°C)
T^*	reference temperature (often 25C°or 298K).
V	voltage (V)
Voc	open-circuit voltage (V)

Abreviations

AC	alternative current
ADCU	acquisition data and control unit
CU	central unit
DC	direct current
DDM	double diode model
GUI	graphical user interface
ns	number of cells in series
np	number of cells in parallel
PV	photovoltaic
PVG	photovoltaic generator
SDM	single diode model
SP	series-parallel
STC	standard test conditions
TCT	total-cross-tied
WDS	wireless digital switch- generator
WMC	wireless mini-characterizer

Greek symbols

μ_{ISC}	coefficient of variation of short-circuit current with temperature.